

Published in final edited form as:

*Mol Microbiol.* 2014 January ; 91(1): . doi:10.1111/mmi.12454.

## Differential roles for the Co<sup>2+</sup>/Ni<sup>2+</sup> transporting ATPases, CtpD and CtpJ, in *Mycobacterium tuberculosis* virulence

Daniel Raimunda<sup>1,#</sup>, Jarukit E. Long<sup>2,#</sup>, Teresita Padilla-Benavides<sup>1</sup>, Christopher M. Sassetti<sup>2,3</sup>, and José M. Argüello<sup>1</sup>

<sup>1</sup>Department of Chemistry and Biochemistry, Worcester Polytechnic Institute, Worcester, MA, 01609

<sup>2</sup>Department of Microbiology and Physiological Systems, University of Massachusetts Medical School, Worcester, MA, 01655

<sup>3</sup>Howard Hughes Medical Institute, Chevy Chase, MD, 20815

### SUMMARY

The genome of *Mycobacterium tuberculosis* encodes two paralogous P<sub>1B4</sub>-ATPases, CtpD (*Rv1469*) and CtpJ (*Rv3743*). Both proteins showed ATPase activation by Co<sup>2+</sup> and Ni<sup>2+</sup>, and both appear to be required for metal efflux from the cell. However, using a combination of biochemical and genetic studies we found that these proteins play nonredundant roles in virulence and metal efflux. CtpJ expression is induced by Co<sup>2+</sup> and this protein possesses a relatively high turnover rate. A *ctpJ* deletion mutant accumulated Co<sup>2+</sup>, indicating that this ATPase controls cytoplasmic metal levels. In contrast, CtpD expression is induced by redox stressors and this protein displays a relatively low turnover rate. A *ctpD* mutant failed to accumulate metal, suggesting an alternative cellular function. *ctpD* is co-transcribed with two thioredoxin genes *trxA* (*Rv1470*), *trxB* (*Rv1471*), and an enoyl-coA hydratase (*Rv1472*), indicating a possible role for CtpD in the metallation of these redox-active proteins. Supporting this, *in vitro* metal binding assays showed that TrxA binds Co<sup>2+</sup> and Ni<sup>2+</sup>. Mutation of *ctpD*, but not *ctpJ*, reduced bacterial fitness in the mouse lung, suggesting that redox maintenance, but not Co<sup>2+</sup> accumulation, is important for growth *in vivo*.

### Keywords

CtpD; CtpJ; Co<sup>2+</sup>-ATPase; redox stress; metal loading; virulence

### INTRODUCTION

Upon infection, *Mycobacterium tuberculosis* replicates within a phagosome-like compartment of the host macrophage (Aderem & Underhill, 1999, Vergne *et al.*, 2004, Flynn & Chan, 2001). Transition metal homeostasis (namely Cu<sup>+2+</sup>, Zn<sup>2+</sup>, Fe<sup>2+/3+</sup> and Mn<sup>2+</sup>) can alter the outcome of this interaction by numerous mechanisms (Hood & Skaar, 2012, Rowland & Niederweis, 2012, Forbes & Gros, 2001, Argüello *et al.*, 2011). Increased Cu<sup>+</sup> and Zn<sup>2+</sup> and decreased Fe<sup>2+</sup> concentrations, have been described in phagosomes of interferon-gamma activated macrophages (Wagner *et al.*, 2006). These alterations, in conjunction with the activation of the phagosomal inducible nitrogen oxide synthase (iNOS) and NADPH oxidase, lead to bacterial clearance (Vergne *et al.*, 2004, Flynn & Chan, 2001).

To whom correspondence should be addressed: José M. Argüello, Department of Chemistry and Biochemistry, Worcester Polytechnic Institute, 100 Institute Road, Worcester, MA, USA, Tel: (508) 831-5326; Fax: (508) 831-4116; arguello@wpi.edu.

<sup>#</sup>Both authors contributed equally to this work.

The pathogen adapts to this environment through the use of specific metal transporters. Transition metals are essential micronutrients, as they are co-factors in bacterial metalloenzymes necessary for various metabolic processes and coping with redox stress. As a result metal importers are required for bacterial virulence in a number of systems (Rowland & Niederweis, 2012, Forbes & Gros, 2001, Argüello et al., 2011, Botella *et al.*, 2011, Padilla-Benavides *et al.*, 2013). However, at high concentrations these metals can also be cytotoxic, and bacterial efflux systems are equally important for growth in the host environment. Consequently, *M. tuberculosis* infection is dependent on maintaining appropriate transition metal homeostasis.

The *M. tuberculosis* genome possesses an unusually high number of heavy metal transporting P<sub>1B</sub>-type ATPases<sup>1</sup>. Members of this family of proteins are characterized by a highly conserved core protein structure and a common mechanism of transport (Argüello *et al.*, 2007, Argüello et al., 2011). These can be classified into distinct subgroups, clustered by conserved transmembrane metal binding sites (TM-MBS) and consequent metal specificity (Argüello, 2003). P<sub>1B</sub>-ATPases export cytosolic transition metals as part of metal excess responsive systems, and control cellular metal quotas (Raimunda *et al.*, 2011). Moreover, emerging new data suggest that some P<sub>1B</sub>-ATPase are part of the redox tolerance machinery of intracellular pathogens, as they participate in the assembly of membrane and secreted redox metalloenzymes (Argüello et al., 2011, González-Guerrero *et al.*, 2010, Osman *et al.*, 2013, Padilla-Benavides et al., 2013). These represent a novel function for metal transporters; i.e., they are also part of metalloprotein assembly systems. More importantly, this has notable implications for the conceptual development of metal homeostasis models. This is, transition metals although not free are transported to specific target metalloproteins that from a system perspective operate as metal pool/compartments. The identification of additional examples, in particular with novel and unique metal specificities, validates the general importance of this mechanistic strategy.

The involvement of *M. tuberculosis* P<sub>1B</sub>-ATPases CtpV (Rv0969) and CtpC (Rv3270) in Cu<sup>+</sup> and Mn<sup>2+</sup> homeostasis and virulence has been shown (Ward *et al.*, 2010, Botella et al., 2011, Padilla-Benavides et al., 2013). In addition, a previous genomic analysis directed to identify genes essential for *M. tuberculosis* growth during infection showed the requirement of *ctpD* (Rv1469) for *in vivo* survival fitness (Sasseti & Rubin, 2003). CtpD is a member of the Co<sup>2+</sup>/Ni<sup>2+</sup>-transporting P<sub>1B4</sub>-ATPase sub-group (Argüello, 2003, Rutherford *et al.*, 1999, Raimunda *et al.*, 2012a, Zielazinski *et al.*, 2012). Characterization of the *M. smegmatis* homolog (*MSMEG\_5403*) showed that it transports Co<sup>2+</sup> and Ni<sup>2+</sup> and its transcription was induced by Co<sup>2+</sup> (Raimunda et al., 2012a). In agreement with this, mutations in *M. smegmatis* Co<sup>2+</sup>-ATPase led to an increase in intracellular Co<sup>2+</sup> and Ni<sup>2+</sup> levels. Additionally, an increase in susceptibility to these metals was observed (Raimunda et al., 2012a). While maintaining cytoplasmic Co<sup>2+</sup> and Ni<sup>2+</sup> levels appears as a simple parsimonious role for this subtype of ATPases, this model is complicated by the presence of two homologous P<sub>1B4</sub>-ATPase coding genes, *ctpD* and *ctpJ*, in several Mycobacterium species including *M. tuberculosis* (Fig. 1A and 1B). The presence of two paralogous P<sub>1B4</sub>-ATPases was also observed in *Gramella forsetii*, *Oligotropha carboxidovorans* OM5, and *Xanthobacter autotrophicus* (Raimunda et al., 2012a). All these proteins present a large cytoplasmic ATP binding and hydrolysis domains and six transmembrane fragments (TM) containing metal binding residues S in TM4, and HEXXT in TM6 (Argüello, 2003, Raimunda et al., 2012a, Zielazinski et al., 2012).

<sup>1</sup>For simplicity P-type ATPases will be referred as P-ATPases, P<sub>1B</sub>-ATPases, etc.

CtpD and CtpJ homologs from various mycobacteria are closely related at the primary sequence level (Fig. 1A). However, the genes flanking *ctpD/J* homologs are distinct and this genomic context can be used to assign orthology (Fig. 1B and C). The  $\text{Co}^{2+}$  sensing transcriptional regulator *nmtR*, is always upstream of *ctpJ* orthologs. *nmtR* is a member of the ArsR-SmtB family of transcriptional repressors (Cavet *et al.*, 2002). The *ctpD* orthologs are found together with two thioredoxins - *trxA* (*Rv1470*) and *trxB* (*Rv1471*) - and a putative enoyl-CoA hydratase (*Rv1472*) coding genes downstream (Fig. 1C). Unlike TrxB and TrxC, *in vitro* functional studies have shown that TrxA has an unusual low redox potential and is not functional in the presence of *M. tuberculosis* thioredoxin reductase (TrxR) (Akif *et al.*, 2008). Although bioinformatics analysis suggests that *ctpD* transcription is monocistronic (<http://www.tbdb.org/>), it is notable that *trxA* is always present in the same position next to *ctpD* and is absent in all *Mycobacterium* species missing the *ctpD* homolog. Adding to these correlations, a proteomic study combining cellular fractionation and 2D-LC MS/MS showed the co-localization of CtpD, TrxA and the enoyl-CoA-hydratase in the membrane fraction (Mawuenyega *et al.*, 2005).

Considering the different physiological functions observed in homologous  $\text{P}_{1\text{B}}$ -ATPases (Argüello *et al.*, 2011, Padilla-Benavides *et al.*, 2013, González-Guerrero *et al.*, 2010, Osman *et al.*, 2013), the presence of CtpD and CtpJ in *M. tuberculosis* presents a unique opportunity to demonstrate the broad application of a strategy to employ pairs of metal transporters with similar specificity but different kinetics characteristics, to transport metal to different targets. This general model was tested in comparative *in vivo* and *in vitro* analyses. *In vivo* experiments confirmed the requirement of *ctpD*, but not *ctpJ*, for virulence. Biochemical analysis showed identical metal specificity and transport direction for both ATPases, although they work at different rates. These biochemical characteristics were in agreement with cellular metal accumulation assays and expression profiles under different stress conditions. The data suggest that while CtpJ is responsible for maintaining  $\text{Co}^{2+}$  cytoplasmic level; CtpD plays a unique role in redox stress response and adapting to the host environment. Furthermore, the co-transcription of CtpD with thioredoxins, their previously demonstrated co-localization, and the specific binding of  $\text{Co}^{2+}$  to TrxA, suggest that CtpD participates in the metallation of cobaloproteins.

## RESULTS

### CtpD and CtpJ transport $\text{Co}^{2+}$ and $\text{Ni}^{2+}$ at different rates

*M. tuberculosis* CtpD and CtpJ sequences contain conserved amino acids present in homologous proteins that are selective for  $\text{Co}^{2+}$  and  $\text{Ni}^{2+}$  transport (Raimunda *et al.*, 2012a, Zielazinski *et al.*, 2012).  $\text{P}_{1\text{B}}$ -ATPases couple substrate transport across membranes to ATP hydrolysis following the Albers-Post E1/E2-like mechanism (Argüello *et al.*, 2007). Both proteins were expressed in *E. coli* and affinity purified (Fig 2A), to confirm their metal specificity and analyze their enzymatic characteristics. Protein preparations were incubated with TEV protease and then pre-treated with chelating agents before metal dependent ATP hydrolysis was measured (Raimunda *et al.*, 2012a). It is important to note that  $\text{P}_{1\text{B4}}$ -ATPases lack amino- and carboxyl-terminus MBDs (N-, C- MBD) (Argüello, 2003) and that treatment of the protein with TEV protease removes the (His)<sub>6</sub>-tag used during in enzyme purification (Fig. 2A).  $\text{Co}^{2+}$  and  $\text{Ni}^{2+}$  activated CtpD and CtpJ ATPase activity in the  $\mu\text{M}$  range (Fig. 2B and 2C). Other transition metals such as  $\text{Zn}^{2+}$ ,  $\text{Cu}^{+2+}$ ,  $\text{Mn}^{2+}$  and  $\text{Fe}^{2+}$  in concentrations ranging from nM to mM failed to activate the enzyme (data not shown). Importantly, CtpD showed a 4- fold lower  $V_{\text{max}}$  compared to CtpJ in presence of either substrate. This was also matched by slightly higher affinity of CtpD for the metal when compared to CtpJ. The  $V_{\text{max}}$  value for both metals observed for CtpJ, resembles the biochemical behavior of *M. smegmatis*  $\text{Co}^{2+}$ -ATPase that we designate as its ortholog (Fig. 1). The different

biochemical kinetics (low vs. high transport rate of CtpD vs. CtpJ), suggests that while CtpJ might control the cytosolic metal levels, CtpD could be required for additional physiological functions, as seen with other P<sub>1B1</sub>-ATPases (González-Guerrero et al., 2010, Raimunda et al., 2011, Osman et al., 2013).

### CtpD and CtpJ bind cytoplasmic metals

Previous reports on P<sub>1B4</sub>-ATPases have shown that these enzymes drive the efflux of cytoplasmic Co<sup>2+</sup> (Rutherford et al., 1999, Raimunda et al., 2012a). The binding of the metal substrate to the TM-MBS facing the intracellular side is a well-known requisite for ATP hydrolysis by P<sub>1B</sub>-ATPases (Argüello et al., 2007, Raimunda et al., 2011). Nevertheless, it can be argued that CtpD or CtpJ might drive Co<sup>2+</sup>/Ni<sup>2+</sup> influx and ATP hydrolysis is associated with the efflux of an alternative substrate. This would imply Co<sup>2+</sup>/Ni<sup>2+</sup> binding to CtpD or CtpJ in the E2 conformation, *i.e.*, exposing the TM-MBS to the extracellular space. Vanadate stabilizes P-ATPases in E2 conformation (Pick, 1982, Eren & Argüello, 2004). Thus, to evaluate the direction of transport the metal binding of Co<sup>2+</sup> and Ni<sup>2+</sup> to CtpD and CtpJ was measured in the absence or presence of vanadate. Incubation of each (His)<sub>6</sub>-less protein with the metals in a molar ratio 1:10 showed a TM-MBS binding stoichiometry of approximately 1:1 molar ratio in agreement with previous reports (Zielazinski et al., 2012, Raimunda et al., 2012a) (Table 2). This binding was largely abolished in the presence of 1.5 mM vanadate. The inhibition of metal binding observed in both proteins can be mechanistically explained considering the displacement of the E1/E2 equilibrium towards the E2 state (TM-MBS exposed to the extracellular side) preventing binding to the E1 form. Based on these data, we conclude that both proteins drive the efflux of the cytoplasmic substrate.

### Deletion of *ctpD* and *ctpJ* cause opposing alterations in cellular Co<sup>2+</sup> levels

Previously described P<sub>1B</sub>-ATPases have been mostly associated with maintaining cytoplasmic transition metal levels (Argüello et al., 2011, Argüello et al., 2007, Osman & Cavet, 2008). However, in the human opportunistic pathogen *Pseudomonas aeruginosa*, the two paralogous genes coding for Cu<sup>+</sup> transporting ATPases show no redundancy in their functional roles. One gene is involved in Cu<sup>+</sup> homeostasis (CopA1) while the other participates in metalloprotein biogenesis (CopA2) (González-Guerrero et al., 2010). Considering the possibility of similar alternative roles for *M. tuberculosis* P<sub>1B4</sub>-ATPases, their involvement in maintaining cellular metal quotas was tested. Wild-type, single *ctpD::hyg* and *ctpJ::hyg* mutants, and the double mutant *ctpD-ctpJ::hyg* strains were challenged by supplementing 7H9-OADC media with various metals and the resulting cellular metal levels were determined. A significant decrease of Co<sup>2+</sup> content was observed in the *ctpD::hyg* mutant, whereas Co<sup>2+</sup> accumulated in *ctpJ::hyg* and *ctpD-ctpJ::hyg* double mutant strains when compared to the wild-type (Fig. 3A). Complemented mutant strains showed metal contents similar to those of wild-type cells. No significant differences were observed in Ni<sup>2+</sup> or Cu<sup>2+</sup>-challenged cells (Fig 3B and 3C). These results, together with the biochemical kinetic parameters observed in the purified preparations of CtpJ (Fig 2B), support the hypothesis that CtpJ is responsible for maintaining cytoplasmic Co<sup>2+</sup> (but not Ni<sup>2+</sup>) levels. CtpD appears to have an alternative role since deletion of the coding gene does not lead to an increase but rather a decrease in cytoplasmic Co<sup>2+</sup> level. As shown below this is likely due to a compensatory increase of *ctpJ* expression in the *ctpD* mutant. It is also notable that CtpD is not able to complement the *ctpJ* defect probably because of its slow turnover rate. Additional experiments exploring the tolerance of *ctpD* and *ctpJ* mutant cells to Co<sup>2+</sup>, Ni<sup>2+</sup>, Cu<sup>2+</sup>, and Zn<sup>2+</sup> showed no differences between these and the wild-type strain (data not shown).

### Expression of *ctpD* and *ctpJ* is induced by different stressors

*M. tuberculosis* manages to survive in the hostile phagosomal environment through to its ability to adapt to changes in pH, transition metal bioavailability, redox stress, and nutritional starvation (Ehrt & Schnappinger, 2009, Rowland & Niederweis, 2012). Toward elucidating the mechanism of *ctpD* participation in the infection process, its expression under stress conditions present in the phagosome and upon exposure to various metals was studied. Sub-lethal concentrations for  $\text{Co}^{2+}$ ,  $\text{Ni}^{2+}$  and  $\text{Zn}^{2+}$  were chosen from metal sensitivity assays (Suppl. Fig. 1). None of the tested metals induced *ctpD* expression (Fig. 4A). On the other hand, in a similar manner to the *M. smegmatis* ortholog, expression of *ctpJ* in *M. tuberculosis* was induced by the presence of  $\text{Co}^{2+}$  (Fig. 4B) (Raimunda et al., 2012a, Cavet et al., 2002). Addition of  $\text{Ni}^{2+}$  to the media did not induce the transcription of *ctpD* or *ctpJ* (Fig 4A, B). Among a battery of tested redox stressors, Nitroprusside and potassium cyanide (KCN) increased *ctpD* expression 10- and 7-fold, respectively (Fig. 4A). Nitroprusside, Triclosan and Tert-butyl hydroperoxide (TBHP) also led to induction of *ctpJ* transcription, although these were smaller than the induction by  $\text{Co}^{2+}$  (Fig. 4B).

The lack of *ctpD* induction by metals might be a consequence of the media used, as 7H9 contains significant amounts of  $\text{Cu}^{2+}$  and  $\text{Zn}^{2+}$ . Similarly, lack of *ctpJ* Ni induction could be due to  $\text{Ni}^{2+}$  presence. Therefore, we tested the response to  $\text{Cu}^{2+}$ ,  $\text{Zn}^{2+}$ ,  $\text{Co}^{2+}$  and  $\text{Ni}^{2+}$  of *ctpD* and *ctpJ* transcription in cells grown in Sauton's media treated with Chelex. This treatment decreased metal levels to sub-nM concentrations as measured by AAS (not shown). None of the metals tested induced *ctpD* transcription (Fig. 4C). Unexpectedly, its transcription was decreased by  $\text{Zn}^{2+}$ . Like in 7H9 media, *ctpJ* was induced only by  $\text{Co}^{2+}$  (Fig. 4D). Since CtpD and CtpJ are highly homologous and are both capable of binding and transporting  $\text{Co}^{2+}$ , a compensatory induction of one ATPase in a mutant lacking the other might be hypothesized. No induction of *ctpD* was observed in the *ctpJ::hyg* mutant strain (relative expression was  $0.55 \pm 0.01$  fold, relative to that observed in the wild-type cells). Alternatively, when *ctpJ* expression was analyzed in the *ctpD::hyg* cells a  $3.6 \pm 0.6$  fold induction was observed (Fig. 4E). This induction of *ctpJ* in the *ctpD::hyg* mutant strain likely explains the decrease in intracellular  $\text{Co}^{2+}$  observed in these cells (Fig. 3A).

### *ctpD* is co-transcribed with thioredoxin A, B, and an enoyl-CoA hydratase under reactive nitrogen species (RNS) stress

The described data support the role of CtpD as a  $\text{Co}^{2+}$ -ATPase distinct from CtpJ, but did not reveal the role of this enzyme. *ctpD*'s genetic environment was considered in the search for clues on its role (Fig. 1C). Genetic studies have shown that in *M. tuberculosis* *ctpD* and *trxA* are under regulation of the stress-responsive sigma factor SigF. *M. tuberculosis* *sigF* is induced under stress conditions such as nutrient starvation, macrophage infection, or stationary phase entry (Williams et al., 2007). Searching for a molecular/functional link between these genes, we evaluated whether or not *ctpD* is part of a contiguous operon co-transcribed with down-stream genes under stress conditions (Fig. 1C). RNA extracted from cells challenged for 2 h with Nitroprusside was reverse-transcribed and the operon was mapped by PCR. Fig. 5 shows that *ctpD* is co-transcribed in a single operon together with *trxA*, *trxB*, and *echA12*, an enoyl-CoA hydratase, suggesting the participation of these genes in a coordinated response.

### TrxA binds specifically $\text{Co}^{2+}$ and $\text{Ni}^{2+}$

The co-transcription of *trxA* and *ctpD* together with their co-localization (Mawuenyega et al., 2005), and the low turnover rate of CtpD suggest that TrxA could be a CtpD's client protein in the extracellular side of the membrane. In this way TrxA would be capable of accepting  $\text{Co}^{2+}/\text{Ni}^{2+}$  as a metal chaperone or a redox buffer/operator. To test this, metal binding to heterologously expressed and purified TrxA was assayed. Prior to this, the  $(\text{His})_6$ -



tag used for purification was removed from TrxA by TEV treatment (Fig. 6A). TrxA was capable of  $\text{Co}^{2+}$  and  $\text{Ni}^{2+}$  binding under reducing conditions with a stoichiometry of 2:1 (Fig. 6B). This binding appeared specific for these metals since the protein could not bind  $\text{Zn}^{2+}$ .

### ***ctpD* is required for the growth of *M. tuberculosis* in mouse lung**

Previous whole genome genetic screens suggested that *ctpD* but not *ctpJ* may be required for the growth or survival of *M. tuberculosis* during infection (Sasseti & Rubin, 2003). To verify this prediction, we directly determined the relative fitness of these mutants in a competitive infection assay. Mice were infected with a mixture of wild-type and mutant bacteria and the relative fitness of each strain was estimated by determining the change in ratio (mutant/wild-type) in mouse lungs over time (Fig. 7). Over a 28 day infection the representation of the *ctpD::hyg* mutant decreased by 10-fold. In contrast, the *ctpJ::hyg* strain and the complemented *ctpD::hyg* mutant grew indistinguishably from wild-type *M. tuberculosis*.

## **DISCUSSION**

The  $\text{P}_{1\text{B}}$ -ATPase transition metal transporters are emerging as important determinants of virulence in a variety of intracellular pathogens (Osman *et al.*, 2010, McLaughlin *et al.*, 2012, Raimunda *et al.*, 2011, Padilla-Benavides *et al.*, 2013, Argüello *et al.*, 2011, Botella *et al.*, 2011). Genomes of pathogens frequently contain several  $\text{P}_{1\text{B}}$ -ATPases, with identical metal specificity and direction of transport (Argüello, 2003, Osman *et al.*, 2013, Argüello *et al.*, 2011).  $\text{Co}^{2+}$  transporting  $\text{P}_{1\text{B}4}$ -ATPases are widely distributed in nature (Argüello, 2003, Raimunda *et al.*, 2012a, Rutherford *et al.*, 1999, Zielazinski *et al.*, 2012). However, only some plants and a few bacterial genera, *M. tuberculosis* among them, possess two  $\text{P}_{1\text{B}4}$ -ATPases. Those present in mycobacteria have been referred as CtpD and CtpJ. Previous genetic screens suggested that these proteins serve nonredundant roles during infection (Sasseti & Rubin, 2003). On the other hand, evidence is emerging supporting distinct roles for  $\text{Cu}^{+}$ - and  $\text{Mn}^{2+}$ -ATPases not only in maintaining cytoplasmic metal quotas, but also participating in the assembly of metalloproteins. In this report, we present evidence of the alternative functions played by  $\text{Co}^{2+}$ -ATPases in mechanisms of metal homeostasis and allocation. In particular, we characterize the functional role CtpD, and its singular importance for *M. tuberculosis* virulence.

Recent biochemical studies of bacterial  $\text{P}_{1\text{B}4}$ -ATPases support their role in  $\text{Co}^{2+}$  and possibly  $\text{Ni}^{2+}$  homeostasis (Raimunda *et al.*, 2012a, Zielazinski *et al.*, 2012). *M. tuberculosis* CtpJ and CtpD are structurally homologous to those previously studied. Our results show that both  $\text{Co}^{2+}$  and  $\text{Ni}^{2+}$  trigger the CtpD and CtpJ ATPase activity. The apparent substrate affinities and the relative activation by  $\text{Ni}^{2+}$  and  $\text{Co}^{2+}$  are similar to those previously described (Raimunda *et al.*, 2012a, Zielazinski *et al.*, 2012). However, metal accumulation experiments performed in *M. smegmatis* (Raimunda *et al.*, 2012a) and *M. tuberculosis* (this study), as well as, induction of gene expression by  $\text{Co}^{2+}$  but not  $\text{Ni}^{2+}$  (Raimunda *et al.*, 2012a, Rutherford *et al.*, 1999) strongly indicate that these enzymes transport  $\text{Co}^{2+}$  rather than  $\text{Ni}^{2+}$  *in vivo*. The lack of CtpJ induction by  $\text{Ni}^{2+}$  appears to be at odds with previous LacZ reporter studies, which concluded that the operator-promoter region of *ctpJ* is driven by NmtR in mycobacterial cells grown with  $\text{Ni}^{2+}$  (Cavet *et al.*, 2002). However, these studies were performed after much longer (20 h vs. 2 h) exposure to similar metal levels. It is possible that this harsh condition might be eliciting pleiotropic effects leading to gene induction. Although unlikely, in our experimental conditions, a  $\text{Ni}^{2+}$  carryover in cells grown in 7H9 media could mask a transcriptional induction in the Chelex-treated Sauton's media.

*M. tuberculosis* CtpJ maximum activity is comparable to that of the *M. smegmatis* ortholog, although both are much lower (30-fold) than that reported for CoaT from *Sulfitobacter sp. NAS-14.1* (Zielazinski et al., 2012). However, the high activity of CoaT might be exceptional, as it is much higher than any other reported for a transition metal transporter. The even slower turnover rate of CtpD, suggests that this protein might not contribute to maintenance of the cytoplasmic levels of these metals. Metal accumulation experiments support this idea.  $\text{Co}^{2+}$  accumulated in the *ctpJ::hyg* mutant strain, while the *ctpD::hyg* showed a decrease in  $\text{Co}^{2+}$  content (the double *ctpD-ctpJ::hyg* mutant showed  $\text{Co}^{2+}$  levels comparable to the *ctpJ::hyg* mutant). This observation might raise the question of whether CtpD drives metal efflux or influx. Both CtpD and CtpJ, binds the substrate to be exported when intracellular-facing transport sites are available, strongly implying that both act as exporters. Instead, we speculate that the observed compensatory induction of CtpJ expression in the *ctpD::hyg* mutant is responsible for the decreased  $\text{Co}^{2+}$  levels. While *ctpJ* induction might be related to a RNS detoxification-like effect produced by the deletion of *ctpD* (*ctpJ* is induced by Nitroprusside), it also results in a higher  $\text{Co}^{2+}$  exporting capability. This compensatory effect of *ctpD* deletion is reminiscent of the decrease in  $\text{Cu}^+$  content after deletion of  $\text{Cu}^+$ -ATPases likely involved in metallation of cuproproteins rather than maintaining compartmental  $\text{Cu}^+$  levels (Argüello et al., 2011, Raimunda et al., 2011, Tottey et al., 2001).

Surprisingly, the growth of *ctpD::hyg* and *ctpJ::hyg* *M. tuberculosis* strains was not inhibited by  $\text{Co}^{2+}$ . This could be explained on the basis of the heightened capacity of *M. tuberculosis* cells to sense and respond to increases in the bioavailability of  $\text{Co}^{2+}$ . It is known that this function is shared by two transcriptional repressors (Campbell et al., 2007, Cavet et al., 2002). Responses mediated by NmtR lead to *ctpJ* transcriptional induction, while KmtR mediates the induction of *Rv2025c*, a putative cation diffusion facilitator (CDF) transporter (Campbell et al., 2007). NmtR responses are observed at high metal concentrations, whereas KmtR has been detected to act with an extremely high-affinity. In this scenario, and with a high metal content in the sensitivity assay, the *Rv2025c* gene product could be responsible for maintaining tolerable cytoplasmic  $\text{Co}^{2+}$  levels in the absence of CtpJ. While the unique roles of CtpJ and *Rv2025c* remain unclear, their differential regulation, substrate specificity, or energetic requirements are likely to underlie the retention of both in the genomes of many mycobacterial species.

Stringent and hostile conditions met by *M. tuberculosis* in phagosomes induce expression of genes required for fundamental metabolic tasks, such as detoxification of reactive oxygen species (ROS), RNS, and transition metal homeostasis. To this end, physiological stresses faced by *M. tuberculosis* in phagosomes were mimicked *in vitro* and *ctpD* and *ctpJ* expression levels in wild-type strain were analyzed. Among the several stimuli, only Nitroprusside and cyanide induced the *ctpD* transcription (Fig. 4A). Both of these compounds inhibit respiratory chain electron flow and might influence *ctpD* expression by altering cellular redox state.

CopA2, a  $\text{Cu}^+$ -transporting ATPase in *P. aeruginosa*, was shown to be part of an operon containing the *cbb3-1* and *cbb3-2* involved in cytochrome *c* oxidase assembly by supplying  $\text{Cu}^+$  to the catalytic site (González-Guerrero et al., 2010, Hassani et al., 2010). The observed connections between *ctpD* and *trxA* in mycobacteria lead us to analyze the possibility that these genes are part of the same operon and the potential functional link between them. Using RNA obtained from cells grown under nitrosative stress, we determined the co-transcription of *ctpD* with *trxA*, *trxB*, and *echA12*. To understand if *M. tuberculosis* TrxA is a metalloprotein that could be loaded by an ATPase such as CtpD, we assayed its metal binding capability. Under reducing conditions with TCEP, the protein was able to bind  $\text{Co}^{2+}$  and  $\text{Ni}^{2+}$ , but not  $\text{Zn}^{2+}$ , in a protein:metal ratio of 2:1 (Fig. 6B). Although differential

competition for the metal between TCEP and TrxA cannot be discarded, its divalent metal adducts have similarly low stabilities. This, along with the identification of *ctpD*, *trxA*, and *echA12* gene products in membrane fractions, suggests a coordinated function, perhaps a role in lipid membrane metabolism (Mawuenyega et al., 2005). However, the participation of transition metals as co-factors of enoyl-CoA hydratases is unknown (Agnihotri & Liu, 2003) and *trxA* has been reported to be non-functional (Akif et al., 2008), although this could be due to inappropriate protein maturation. Interestingly, a recent report identifying virulence factors in *P. aeruginosa* proposed an enoyl-CoA hydratase to be relevant for infection of *Caenorhabditis elegans*. Its participation in a fatty acid synthesis is likely required for membrane signaling and quorum sensing (Feinbaum et al., 2012). A similar mechanism might be present in *M. tuberculosis*. The study of these hypothetical links is beyond the scope of the work presented here.

Finally, the requirement of CtpD and CtpJ for *M. tuberculosis* virulence was evaluated in a competition (mutant vs. wild-type) infection model. Consistent with previous genomic screens using transposon libraries, our results highlight the importance of *ctpD*, but not *ctpJ*, during *M. tuberculosis* infection (17). Mixed competition assays are useful in determining relative fitness and have been used to demonstrate indispensability of  $Zn^{2+}$  transport systems in *Haemophilus influenza* (Rosadini et al., 2011). The lack of CtpJ participation in virulence is not surprising considering that no apparent changes in  $Co^{2+}$  (or  $Ni^{2+}$ ) levels in activated phagosomes have been reported (Wagner et al., 2005). So why are *ctpD* mutants attenuated during infection? The decreased levels of  $Co^{2+}$  found in the *ctpD* mutant strongly argues against toxicity due to metal accumulation in the bacterial cell. Instead, the putative involvement of CtpD in the response to redox stress in the phagosome might explain why CtpD is required for virulence (Vergne et al., 2004, Flynn & Chan, 2001). CtpD's co-transcription with *trxAB* and *echA12* may suggest that CtpD plays a role in activating these proteins through metallation, protecting *M. tuberculosis* from redox stress. CtpD may also play a role in activating other proteins required for growth.

In this study, we have characterized the functional roles of two *M. tuberculosis*  $P_{1B4}$ -ATPases and established their requirement for the infection process. CtpJ is in charge of cytosolic  $Co^{2+}$  and  $Ni^{2+}$  levels and is dispensable for infection. CtpD appears necessary for metallation of secreted proteins and for overcoming redox stress, reflecting its requirement in *M. tuberculosis* to strive in the harsh environmental phagosome conditions. It remains to be elucidated the participation of CtpD in fatty acid synthesis, plasma membrane lipid remodeling, or signaling processes during lung colonization.

## EXPERIMENTAL PROCEDURES

### Recombeneering, Mutant and Complemented Strains Preparation

Deletion mutants were prepared in the background of the *M. tuberculosis* H37Rv wild-type strain using primers listed in Table 1 according to standard protocols (van Kessel & Hatfull, 2007). For *ctpD* mutation, a 1000 bp fragment corresponding to the 5'-first 500 bp and 3'-last 500 bp of the *ctpD* gene was designed using tuberculist (<http://tuberculist.epfl.ch>). These regions included 30 bp that flanked upstream and downstream of *ctpD* gene. Additionally, an insertion cassette containing the restriction sites for SpeI-HpaI-AscI was added between the 5'- and 3'-500 bp regions. The resulting synthesized fragment was then inserted in a HindIII site into a pUC57 expression vector (GenScript), resulting in pEL2a. Vector pKM342 contains a hygromycin resistance (*hygR*) cassette flanked by SpeI-AscI sites. To insert the *hygR* cassette in pEL2a, both pEL2a and pKM342 were digested with SpeI-AscI. The 1.2 kbp hygromycin fragment was then ligated into pEL2a, resulting in pEL2b. To generate the deletion mutant of *ctpJ* two 500 bp amplicons corresponding to the 5'-first 400 bp plus 100 bp upstream, and the 3'-last 400 bp plus 100 bp downstream of the *ctpJ* gene



were obtained by PCR. These were ligated in pJM1 flanking a *hygR* cassette resulting in pJM1-J. To generate *ctpD* and *ctpJ* mutants, the resulting 2.2 kbp *ctpD-hygR-ctpD* fragment from digestion of pEL2b with HindIII and the 2.8 kbp *ctpJ-hygR-ctpJ* generated by PCR using as template pJM1-1 plasmid, were both transformed into *M. tuberculosis* H37Rv recombineering strain. Briefly, the *M. tuberculosis* H37Rv recombineering strain bearing plasmid pJV53 was grown till  $OD_{600}=0.7$  and incubated for 18 h with 1  $\mu$ M isovaleronitrile. The culture was treated with 0.2 M glycine for 8 h before making electrocompetent cells. The recombineering strain was electroporated and selected by hygromycin resistance on 7H10 plates. After 18 days, *hygR* colonies were isolated and transferred to 2 ml inkwells containing 7H9 media supplemented with 50  $\mu$ g/ml hygromycin. To verify the presence of the *ctpD* and *ctpJ* deletion mutation, PCR amplification of the *hygR* cassette flanked by the N- and C- terminals was performed. The double mutant was obtained as described above for *ctpJ*, although using a cleaned-up hygromycin sensitive *ctpD* mutant as parental strain.

The complementation assay constructs were made by amplifying *M. tuberculosis ctpD* and *ctpJ* from genomic DNA. The resulting PCR fragments were digested and ligated into pJEB402 which confers kanamycin resistance (*kanR*) resulting in pJEB402-D and pJEB402-J. The ligation reactions were transformed into DH5 $\alpha$  cells and the presence of the insert was verified by colony PCR and restriction digests. The plasmids were then purified and transformed into the *ctpJ* and *ctpD* *M. tuberculosis* mutant strains. Transformants showing *kanR* were analyzed for the presence of *ctpD* and *ctpJ* by PCR.

### Mice Infection

The relative growth rates of *M. tuberculosis* H37Rv wild-type and *ctpD::hyg* and *ctpJ::hyg* mutant strains, were examined *in vivo* competition experiments. Briefly, the two strains were mixed with wild-type H37Rv in approximately 3:1 (wild-type:*ctpD::hyg* or wild-type:*ctpJ::hyg* mutants) ratio (final volume 200  $\mu$ l), containing  $6 \times 10^5$  CFU and were inoculated into the tail vein of female C57BL/6J mice. Groups of three mice were sacrificed at indicated time points and the bacterial burden in the lung homogenates were obtained by plating on 7H10 agar medium with or without 100  $\mu$ g/ml hygromycin for mutants CFU and total CFU counting, respectively. A Competitive Index was calculated as  $(CFU_{WT}/CFU_{mutant})_{output}/(CFU_{WT}/CFU_{mutant})_{input}$ . Mice were housed under specific pathogen-free conditions and in accordance with the University of Massachusetts Medical School, IACUC guidelines.

### Protein Expression and Purification

cDNA encoding *M. tuberculosis ctpD*, *ctpJ* and *trxA* were amplified using genomic DNA as template and reverse primers that introduced a Tobacco etch virus (TEV) protease site coding sequence at the amplicon 3' ends. The PCR products were cloned into pBAD-TOPO/His (*ctpD*, and *ctpJ*) or pEXP5-CT-TOPO (*trxA*) vector (Invitrogen) that introduce a (His)<sub>6</sub>-tag at the carboxyl end of the protein. cDNA sequences were confirmed by automated sequence analysis. For CtpD and CtpJ expression the constructs were introduced into *E. coli* LMG194  $\Delta copA$  cells (Rensing *et al.*, 2000). For protein expression, cells were grown at 37°C in ZYP-505 media supplemented with 0.05% arabinose, 100  $\mu$ g/ml ampicillin, and 50  $\mu$ g/ml kanamycin (Studier, 2005). Affinity purification of membrane proteins and removal of the (His)<sub>6</sub>-tag was performed as previously described (Mandal *et al.*, 2002, Raimunda *et al.*, 2012b). Solubilized lipid/detergent micellar forms of CtpD and CtpJ proteins were stored at -20°C in buffer containing 25 mM Tris, pH 8.0, 50 mM NaCl, 0.01% n-dodecyl- $\beta$ -D-maltopyranoside (DDM) (Calbiochem), and 0.01% alectin until use. TrxA was expressed in BL21 (DE3)pLysS cells transformed with pEXP5-CT-TrxA following the protocol described previously (Akif *et al.*, 2008). Protein determinations were performed in accordance to Bradford (Bradford, 1976). Protein purity was assessed by Coomassie Brilliant

Blue (CBB) staining of overloaded SDS-PAGE gels and by immunostaining Western blots with rabbit anti-(His)<sub>6</sub> polyclonal primary antibody (GenScript) and goat anti-rabbit IgG secondary antibody coupled to horseradish peroxidase (GenScript). Previous to ATPase activity determinations, proteins (1 mg/ml) were treated with 0.5 mM EDTA and 0.5 mM tetrathiomolybdate (TTM) for 45 min at room temperature. Chelators were removed using Ultra-30 Centricon (Millipore) filtration devices.

### ATPase assays

These were performed at 37°C in a medium containing 50 mM Tris (pH 7.4 at RT), 3 mM MgCl<sub>2</sub>, 3 mM ATP, 0.01% asolectin, 0.01% DDM, 20 mM cysteine, 50 mM NaCl, 2.5 mM DTT, and 10–40 mg/ml purified protein plus the indicated metal concentrations. DTT was replaced by TCEP to prevent interference with the colorimetric reaction when Co<sup>2+</sup> activation was measured. ATPase activity was measured after 10 min incubation and released Pi determined according to Lanzetta *et al.* (Lanzetta et al., 1979). ATPase activity measured in the absence of metal was subtracted from plotted values. Curves of ATPase activity versus metal concentrations were fit to  $v = V_{max}[\text{metal}]/([\text{metal}] + K_{1/2})$ . The reported standard errors for  $V_{max}$  and  $K_{1/2}$  are asymptotic standard errors reported by the fitting software KaleidaGraph (Synergy).

### Metal binding determinations

Maximum metal binding to isolated CtpD and CtpJ in the presence (1.5 mM) or absence of vanadate was measured as previously described (Raimunda et al., 2012a). Ten μM CtpD was incubated for 1 min at 4°C in 50 mM HEPES-NaOH, pH 7.5, 200 mM NaCl, 1 mM TCEP, and 50 μM of CoCl<sub>2</sub> or NiCl<sub>2</sub>. After incubation, excess metal was removed by size exclusion using Sephadex G-25 columns (GE Healthcare). Eluted protein was acid digested with 1.25 ml HNO<sub>3</sub> (trace metal grade) for 1 h at 80°C and then overnight at 20°C. Digestion was concluded by addition of 0.25 ml of 30 % H<sub>2</sub>O<sub>2</sub> and dilution to 3 ml with water. Metal binding to TrxA was similarly determined except that Sephadex G-10 columns were used to remove metal excess. Metal content in digested samples was measured by furnace atomic absorption spectroscopy (AAS; Varian SpectraAA 880/GTA 100). Background metal level in control samples lacking protein was < 10% of those observed in protein containing samples.

### Metal Content Analysis

*M. tuberculosis* H37Rv wild-type, the single *ctpD::hyg* and *ctpJ::hyg*, and the double *ctpD-ctpJ::hyg* deletion mutants and complemented strains were grown to the late exponential phase and incubated in the presence or absence of 1 μM CoCl<sub>2</sub>, NiCl<sub>2</sub>, or CuCl<sub>2</sub> for 1 h. After the incubation, cells were washed with 25 mM Tris pH 7.0 and 100 mM KCl and protein levels were determined. Samples were acid digested as described above and metal concentrations measured using furnace AAS.

### Gene expression analysis

*M. tuberculosis* H37Rv wild-type cells in exponential phase in 7H9-OADC were cultured for 2 h with 100 μM Cu<sup>2+</sup>, Zn<sup>2+</sup>, Co<sup>2+</sup>, Ni<sup>2+</sup>, Mn<sup>2+</sup> or Fe<sup>2+</sup> as chloride salts, except for Zn<sup>2+</sup> that was added in the sulfate form. Alternatively cells were exposed to 1 mM Triclosan, a lipid metabolism inhibitor, Nitroprusside, a nitrosative stressor, or the oxidative stressors TBHP, Paraquat, KCN. In alternative experiments, cells grown in Sauton's pre-treated with Chelex (Sigma) (1 g/100 ml) were exposed to 10, 50 and 100 μM of Cu<sup>2+</sup>, Zn<sup>2+</sup>, Co<sup>2+</sup> or Ni<sup>2+</sup>. Cells were harvested, resuspended in 1 ml of TRIzol reagent (Invitrogen), and disrupted using lysing matrix B (MP Biomedicals) in a cell disrupter (FastPrep FP120, Qbiogene). RNA pellets were air dried and redissolved in 50 μl of diethyl pyrocarbonate-treated ultrapure water. Remaining DNA was removed with RNeasy minikit and an on-

column DNase I kit (Qiagen). The RNA samples (1 µg) were used as templates for cDNA synthesis with random primers and SuperScript III reverse transcriptase (Invitrogen). Quantitative reverse transcription-PCR (qRT-PCR) was performed with iQ SYBR green supermix (Bio-Rad Laboratories), using primers listed in Table 1 and cycler conditions previously described (González-Guerrero et al., 2010). The RNA polymerase sigma factor (*sigA*), was used as an internal reference. Determinations were carried out with RNA extracted from three independent biological samples, with the threshold cycle (Ct) determined in triplicate. The relative levels of transcription were calculated by using the  $2^{-\Delta\Delta C_t}$  method (Livak & Schmittgen, 2001). The mock reverse transcription reactions, containing RNA and all reagents except reverse transcriptase, confirmed that the results obtained were not due to contaminating genomic DNAs (data not shown). *ctpD* expression in the *ctpJ* mutant, and vice versa *ctpJ* expression in *ctpD* mutant cells, were measured in cells treated in similar manner

## Supplementary Material

Refer to Web version on PubMed Central for supplementary material.

## Acknowledgments

This work was supported by NIH awards F32A1093049 (J.E.L.), 1R21AI082484 (J.M.A.), AI064282 (C.M.S.) and the Howard Hughes Medical Institute (C.M.S.).

## References

- Aderem A, Underhill DM. Mechanisms of phagocytosis in macrophages. Annual review of immunology. 1999; 17:593–623.
- Agnihotri G, Liu HW. Enoyl-CoA hydratase. reaction, mechanism, and inhibition. Bioorg Med Chem. 2003; 11:9–20. [PubMed: 12467702]
- Akif M, Khare G, Tyagi AK, Mande SC, Sardesai AA. Functional studies of multiple thioredoxins from *Mycobacterium tuberculosis*. J Bacteriol. 2008; 190:7087–7095. [PubMed: 18723612]
- Argüello JM. Identification of ion-selectivity determinants in heavy-metal transport P<sub>1B</sub>-type ATPases. J Membr Biol. 2003; 195:93–108. [PubMed: 14692449]
- Argüello JM, Eren E, González-Guerrero M. The structure and function of heavy metal transport P<sub>1B</sub>-ATPases. Biometals. 2007; 20:233–248. [PubMed: 17219055]
- Argüello JM, González-Guerrero M, Raimunda D. Bacterial transition metal P<sub>1B</sub>-ATPases: transport mechanism and roles in virulence. Biochemistry. 2011; 50:9940–9949. [PubMed: 21999638]
- Botella H, Peyron P, Levillain F, Poincloux R, Poquet Y, Brandli I, Wang C, Tailleux L, Tilleul S, Charriere GM, Waddell SJ, Foti M, Lugo-Villarino G, Gao Q, Maridonneau-Parini I, Butcher PD, Castagnoli PR, Gicquel B, de Chastellier C, Neyrolles O. Mycobacterial P<sub>1</sub>-type ATPases mediate resistance to zinc poisoning in human macrophages. Cell Host Microbe. 2011; 10:248–259. [PubMed: 21925112]
- Bradford MM. A rapid and sensitive method for the quantitation of microgram quantities of protein utilizing the principle of protein-dye binding. Anal Biochem. 1976; 72:248–254. [PubMed: 942051]
- Campbell DR, Chapman KE, Waldron KJ, Tottey S, Kendall S, Cavallaro G, Andreini C, Hinds J, Stoker NG, Robinson NJ, Cavet JS. Mycobacterial cells have dual nickel-cobalt sensors: sequence relationships and metal sites of metal-responsive repressors are not congruent. J Biol Chem. 2007; 282:32298–32310. [PubMed: 17726022]
- Cavet JS, Meng W, Pennella MA, Appelhoff RJ, Giedroc DP, Robinson NJ. A nickel-cobalt-sensing ArsR-SmtB family repressor. Contributions of cytosol and effector binding sites to metal selectivity. J Biol Chem. 2002; 277:38441–38448. [PubMed: 12163508]
- Ehrt S, Schnappinger D. Mycobacterial survival strategies in the phagosome: defence against host stresses. Cell Microbiol. 2009; 11:1170–1178. [PubMed: 19438516]

- Eren E, Arguello JM. Arabidopsis HMA2, a divalent heavy metal-transporting P<sub>1B</sub>-type ATPase, is involved in cytoplasmic Zn<sup>2+</sup> homeostasis. *Plant Physiol.* 2004; 136:3712–3723. [PubMed: 15475410]
- Feinbaum RL, Urbach JM, Liberati NT, Djonovic S, Adonizio A, Carvunis AR, Ausubel FM. Genome-wide identification of *Pseudomonas aeruginosa* virulence-related genes using a *Caenorhabditis elegans* infection model. *PLoS Pathog.* 2012; 8:e1002813. [PubMed: 22911607]
- Flynn JL, Chan J. Immunology of tuberculosis. *Annual review of immunology.* 2001; 19:93–129.
- Forbes JR, Gros P. Divalent-metal transport by NRAMP proteins at the interface of host-pathogen interactions. *Trends Microbiol.* 2001; 9:397–403. [PubMed: 11514223]
- González-Guerrero M, Raimunda D, Cheng X, Argüello JM. Distinct functional roles of homologous Cu<sup>+</sup> efflux ATPases in *Pseudomonas aeruginosa*. *Mol Microbiol.* 2010; 78:1246–1258. [PubMed: 21091508]
- Hassani BK, Astier C, Nitschke W, Ouchane S. CtpA, a copper-translocating P-type ATPase involved in the biogenesis of multiple copper-requiring enzymes. *J Biol Chem.* 2010; 285:19330–19337. [PubMed: 20363758]
- Hood MI, Skaar EP. Nutritional immunity: transition metals at the pathogen-host interface. *Nat Rev Microbiol.* 2012; 10:525–537. [PubMed: 22796883]
- Lanzetta PA, Alvarez LJ, Reinach PS, Candia OA. An improved assay for nanomole amounts of inorganic phosphate. *Anal Biochem.* 1979; 100:95–97. [PubMed: 161695]
- Livak KJ, Schmittgen TD. Analysis of relative gene expression data using real-time quantitative PCR and the 2<sup>(-ΔΔC<sub>T</sub>)</sup> method. *Methods.* 2001; 25:402–408. [PubMed: 11846609]
- Mandal AK, Cheung WD, Arguello JM. Characterization of a thermophilic P-type Ag<sup>+</sup>/Cu<sup>+</sup>-ATPase from the extremophile *Archaeoglobus fulgidus*. *J Biol Chem.* 2002; 277:7201–7208. [PubMed: 11756450]
- Mawuenyega KG, Forst CV, Dobos KM, Belisle JT, Chen J, Bradbury EM, Bradbury AR, Chen X. *Mycobacterium tuberculosis* functional network analysis by global subcellular protein profiling. *Mol Biol Cell.* 2005; 16:396–404. [PubMed: 15525680]
- McLaughlin HP, Xiao Q, Rea RB, Pi H, Casey PG, Darby T, Charbit A, Sleator RD, Joyce SA, Cowart RE, Hill C, Klebba PE, Gahan CG. A putative P-type ATPase required for virulence and resistance to haem toxicity in *Listeria monocytogenes*. *PLoS One.* 2012; 7:e30928. [PubMed: 22363518]
- Osman D, Cavet JS. Copper homeostasis in bacteria. *Adv Appl Microbiol.* 2008; 65:217–247. [PubMed: 19026867]
- Osman D, Patterson CJ, Bailey K, Fisher K, Robinson NJ, Rigby SE, Cavet JS. The copper supply pathway to a *Salmonella* Cu,Zn-superoxide dismutase (SodCII) involves P<sub>1B</sub>-type ATPase copper efflux and periplasmic CueP. *Mol Microbiol.* 2013; 87:466–477. [PubMed: 23171030]
- Osman D, Waldron KJ, Denton H, Taylor CM, Grant AJ, Mastroeni P, Robinson NJ, Cavet JS. Copper homeostasis in *Salmonella* is atypical and copper-CueP is a major periplasmic metal complex. *J Biol Chem.* 2010; 285:25259–25268. [PubMed: 20534583]
- Padilla-Benavides T, Long JE, Raimunda D, Sassetti CM, Arguello JM. A Novel P<sub>1B</sub>-type Mn<sup>2+</sup>-transporting ATPase Is Required for Secreted Protein Metallation in Mycobacteria. *J Biol Chem.* 2013; 288:11334–11347. [PubMed: 23482562]
- Pick U. The interaction of vanadate ions with the Ca-ATPase from sarcoplasmic reticulum. *J Biol Chem.* 1982; 257:6111–6119. [PubMed: 6210692]
- Raimunda D, González-Guerrero M, Leeber BW 3rd, Argüello JM. The transport mechanism of bacterial Cu<sup>+</sup>-ATPases: distinct efflux rates adapted to different function. *Biometals.* 2011; 24:467–475. [PubMed: 21210186]
- Raimunda D, Long JE, Sassetti CM, Argüello JM. Role in metal homeostasis of CtpD, a Co<sup>2+</sup> transporting P<sub>1B4</sub>-ATPase of *Mycobacterium smegmatis*. *Mol Microbiol.* 2012a; 84:1139–1149. [PubMed: 22591178]
- Raimunda D, Subramanian P, Stemmler T, Arguello JM. A tetrahedral coordination of Zinc during transmembrane transport by P-type Zn<sup>2+</sup>-ATPases. *Biochim Biophys Acta.* 2012b; 1818:1374–1377. [PubMed: 22387457]

- Rensing C, Fan B, Sharma R, Mitra B, Rosen BP. CopA: An Escherichia coli Cu(I)-translocating P-type ATPase. Proc Natl Acad Sci U S A. 2000; 97:652–656. [PubMed: 10639134]
- Rosadini CV, Gawronski JD, Raimunda D, Argüello JM, Akerley BJ. A novel zinc binding system, ZevAB, is critical for survival of nontypeable *Haemophilus influenzae* in a murine lung infection model. Infect Immun. 2011; 79:3366–3376. [PubMed: 21576338]
- Rowland JL, Niederweis M. Resistance mechanisms of *Mycobacterium tuberculosis* against phagosomal copper overload. Tuberculosis (Edinb). 2012; 92:202–210. [PubMed: 22361385]
- Rutherford JC, Cavet JS, Robinson NJ. Cobalt-dependent transcriptional switching by a dual-effector MerR-like protein regulates a cobalt-exporting variant CPx-type ATPase. J Biol Chem. 1999; 274:25827–25832. [PubMed: 10464323]
- Sasseti CM, Rubin EJ. Genetic requirements for mycobacterial survival during infection. Proc Natl Acad Sci U S A. 2003; 100:12989–12994. [PubMed: 14569030]
- Studier FW. Protein production by auto-induction in high density shaking cultures. Protein Expr Purif. 2005; 41:207–234. [PubMed: 15915565]
- Totey S, Rich PR, Rondet SAM, Robinson NJ. Two Menkes-type ATPases supply copper for photosynthesis in *Synechocystis* PCC 6803. J Biol Chem. 2001; 276:19999–20004. [PubMed: 11264284]
- van Kessel JC, Hatfull GF. Recombineering in *Mycobacterium tuberculosis*. Nat Methods. 2007; 4:147–152. [PubMed: 17179933]
- Vergne I, Chua J, Singh SB, Deretic V. Cell biology of mycobacterium tuberculosis phagosome. Annual review of cell and developmental biology. 2004; 20:367–394.
- Wagner D, Maser J, Lai B, Cai Z, Barry CE 3rd, Honer Zu, Bentrup K, Russell DG, Bermudez LE. Elemental analysis of *Mycobacterium avium*-, *Mycobacterium tuberculosis*-, and *Mycobacterium smegmatis*-containing phagosomes indicates pathogen-induced microenvironments within the host cell's endosomal system. J Immunol. 2005; 174:1491–1500. [PubMed: 15661908]
- Wagner D, Maser J, Moric I, Vogt S, Kern WV, Bermudez LE. Elemental analysis of the *Mycobacterium avium* phagosome in Balb/c mouse macrophages. Biochem Biophys Res Commun. 2006; 344:1346–1351. [PubMed: 16650826]
- Ward SK, Abomoelak B, Hoyer EA, Steinberg H, Talaat AM. CtpV: a putative copper exporter required for full virulence of *Mycobacterium tuberculosis*. Mol Microbiol. 2010; 77:1096–1110. [PubMed: 20624225]
- Williams EP, Lee JH, Bishai WR, Colantuoni C, Karakousis PC. *Mycobacterium tuberculosis* SigF regulates genes encoding cell wall-associated proteins and directly regulates the transcriptional regulatory gene *phoY1*. J Bacteriol. 2007; 189:4234–4242. [PubMed: 17384187]
- Zielazinski EL, Cutsail GE 3rd, Hoffman BM, Stemmler TL, Rosenzweig AC. Characterization of a Cobalt-Specific P<sub>1B</sub>-ATPase. Biochemistry. 2012; 51:7891–7900. [PubMed: 22971227]



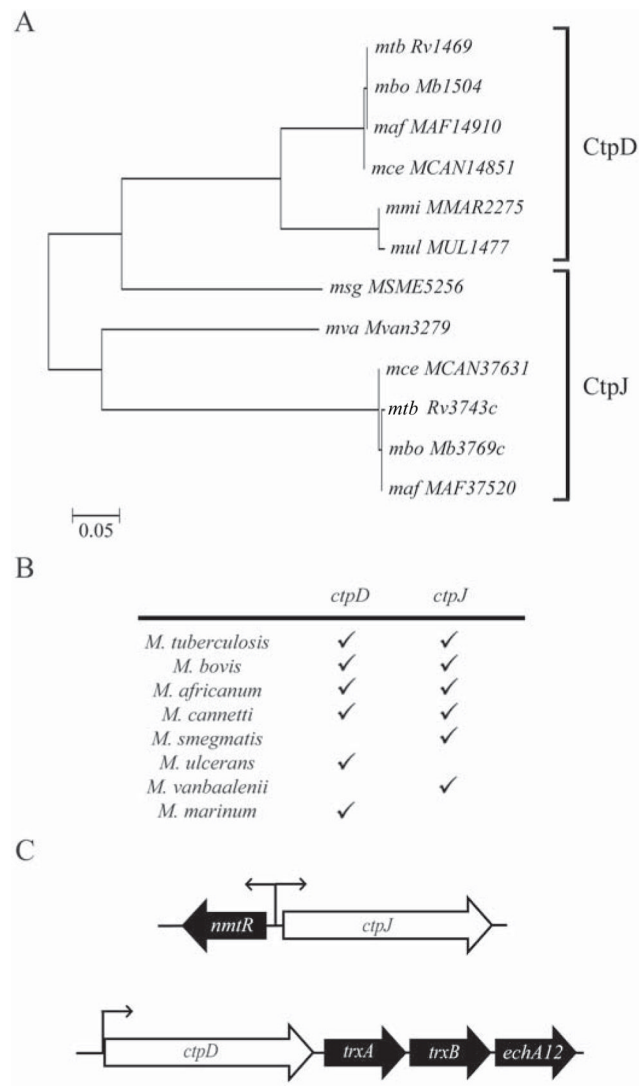


**FIGURE 1. *M. tuberculosis* genome contains two P<sub>1B4</sub>-ATPases codifying genes**  
 (A) Rooted tree of mycobacterial P<sub>1B4</sub>-ATPases obtained from genome-sequenced organisms. (B) Table list describing mycobacterial organisms having *ctpD* and *ctpJ* homologs (check marks indicate the presence of the paralogous gene in that organism). (C) Genetic environment of *M. tuberculosis* *ctpJ* and *ctpD*; arrows represent the DNA regulatory regions.

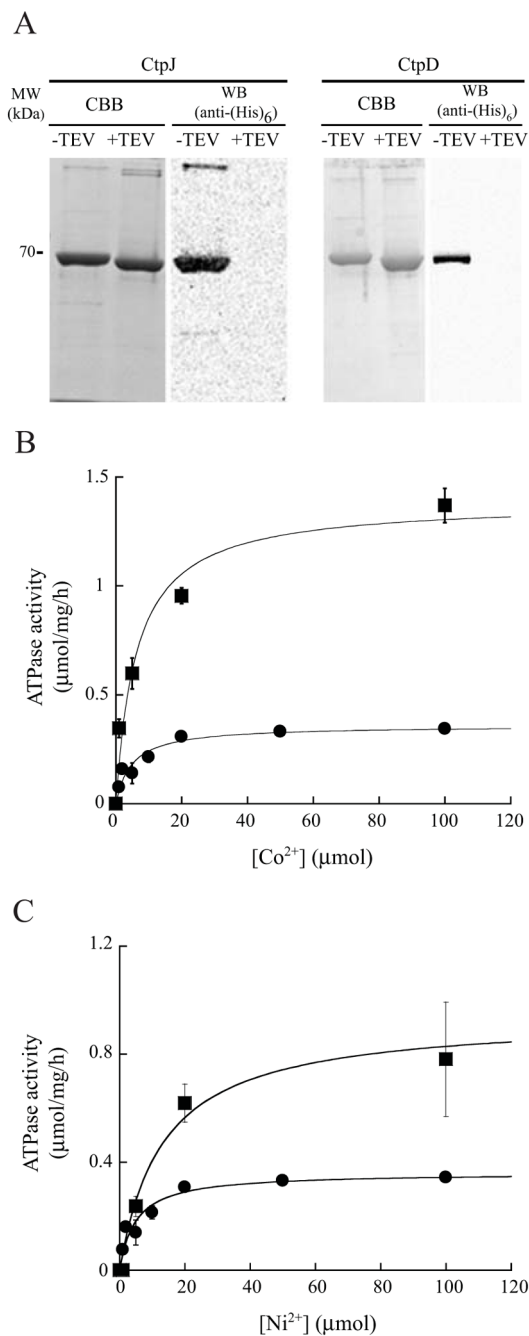


**FIGURE 2. CtpD and CtpJ are Co<sup>2+</sup>/Ni<sup>2+</sup>-ATPases with different transport kinetics**  
 (A) Preparations of Ni-NTA purified CtpD and CtpJ analyzed by Coomassie Brilliant Blue (CBB) and Western blot (WB) using anti-(His)<sub>6</sub> tag antibody. (B) Co<sup>2+</sup> and (C) Ni<sup>2+</sup>-dependent ATPase activity for CtpD (●) and CtpJ (■). Curves of ATPase activity versus metal concentrations were fit to  $v = V_{\max}[\text{metal}]/([\text{metal}] + K_{1/2})$ . Kinetic parameters obtained with Co<sup>2+</sup> for CtpD and CtpJ were  $V_{\max} = 0.35 \pm 0.03 \mu\text{mol/mg/h}$ ,  $K_{1/2} = 4.83 \mu\text{M} \pm 1.4$  and  $V_{\max} = 1.38 \pm 0.12 \mu\text{mol/mg/h}$ ,  $K_{1/2} = 6.3 \pm 2.2 \mu\text{M}$ , respectively. Kinetic parameters with Ni<sup>2+</sup> for CtpD and CtpJ were  $V_{\max} = 0.36 \pm 0.02 \mu\text{mol/mg/h}$ ,  $K_{1/2} = 4.90 \pm 1.18 \mu\text{M}$  and  $V_{\max} = 0.94 \pm 0.05 \mu\text{mol/mg/h}$ ,  $K_{1/2} = 13.23 \pm 2.80 \mu\text{M}$ , respectively. The reported standard

errors for  $V_{\max}$  and  $K_{1/2}$  are asymptotic standard errors reported by the fitting software KaleidaGraph (Synergy). Data are mean  $\pm$  SE (n=3).

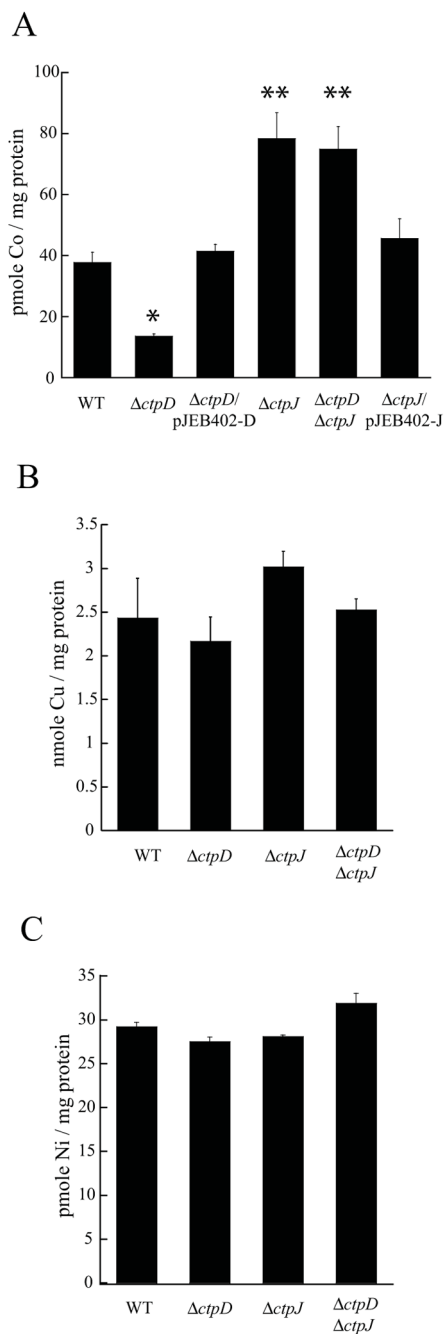


**FIGURE 3. Metal accumulation in *M. tuberculosis* *ctpD::hyg* ( $\Delta ctpD$ ) and *ctpJ::hyg* ( $\Delta ctpJ$ ) mutant strains**

Log-phase cell cultures grown in 7H9-OADC media were supplemented with (A) 100 nM  $\text{Co}^{2+}$ , (B) 3  $\mu\text{M}$   $\text{Cu}^{2+}$  or (C) 1  $\mu\text{M}$   $\text{Ni}^{2+}$  for 2 h. Data represent mean  $\pm$  SE (n=3). \* $p < 0.01$  and \*\* $p < 0.05$  vs. wild-type.

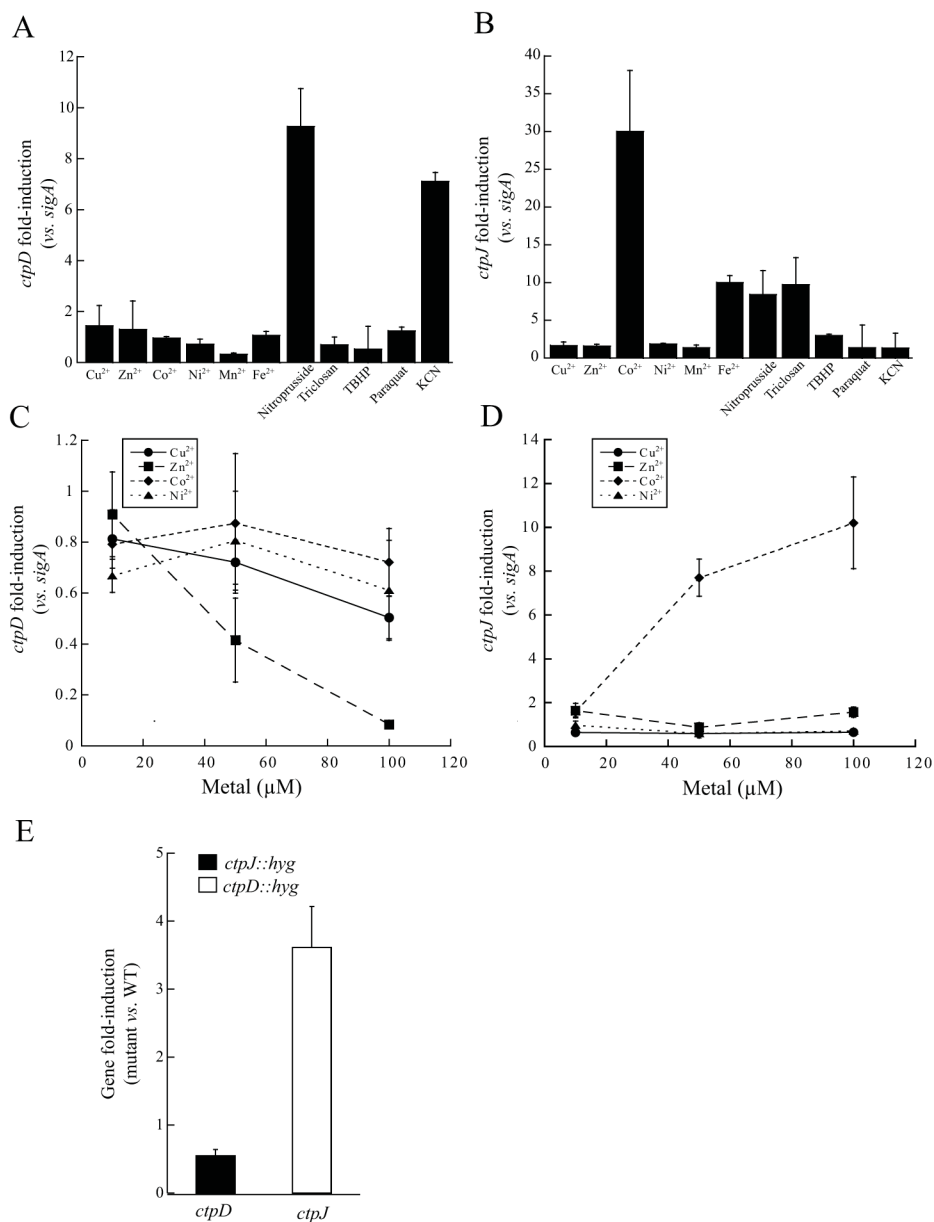


**FIGURE 4. Transcriptional analysis of *ctpD* and *ctpJ* in *M. tuberculosis***

Log-phase H37Rv *M. tuberculosis* cell cultures grown in 7H9-OADC (A, B, E) or chelexed Sauton's (C, D) were supplemented or not, with the indicated metals and redox stressors for 2 h. RNA was extracted and gene expression analyzed for (A, C) *ctpD* or (B, D) *ctpJ* transcriptional induction. (E) *ctpD* and *ctpJ* fold-induction analyzed in *ctpJ::hyg* (black bar) or *ctpD::hyg* (white bar) strains, respectively. Data represent mean  $\pm$  SE (n=3).



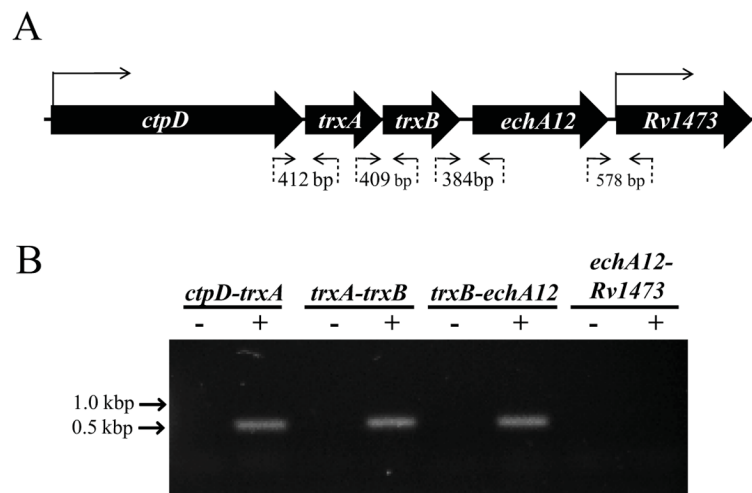


**FIGURE 5. *ctpD* is co-transcribed with *trxA*, *trxB* and *Rv1472* under nitrosative stress**  
 (A) Schematic illustration and (B) representative gel of the *ctpD* operon as determined by RT-PCR using the RNA obtained from *M. tuberculosis* wild-type cells grown under nitrosative stress conditions (1 mM Nitroprusside in 7H9-OADC for 2 h). The location of primers (small arrows) and expected size of the amplification product are indicated. – and + indicate no retro transcribed RNA control and retro transcribed RNA (cDNA), respectively.

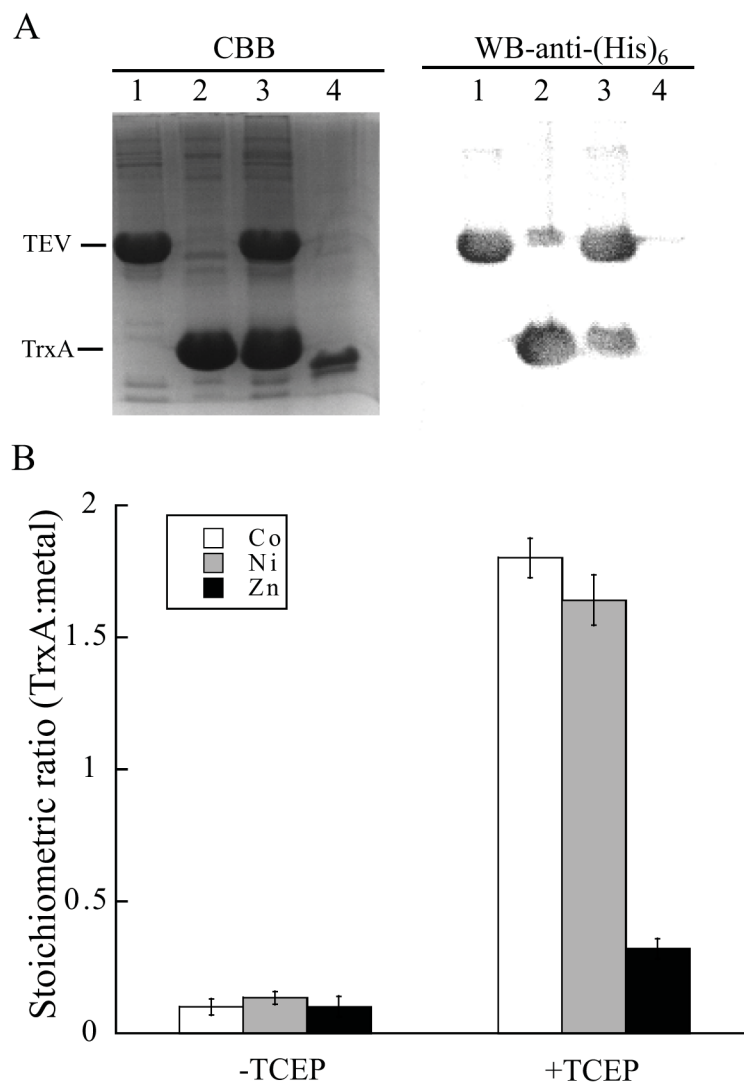


**FIGURE 6. TrxA binds Co<sup>2+</sup> and Ni<sup>2+</sup>**

(A) Coomassie Brilliant Blue (CBB) and immune staining with anti-(His)<sub>6</sub> antibody (WB-anti-(His)<sub>6</sub>) of (1) (His)<sub>6</sub>-TEV, (2) (His)<sub>6</sub>-Tev-TrxA, (3) (His)<sub>6</sub>-Tev-TrxA plus (His)<sub>6</sub>-TEV at time zero and (4) reverse purified (His)<sub>6</sub>-less TrxA after 3 hour incubation. Note that Tev refers to the cleavage site and TEV refers to the protease. (B) Co<sup>2+</sup> (white bars), Ni<sup>2+</sup> (grey bars) or Zn<sup>2+</sup> (black bars) binding to (His)<sub>6</sub>-less TrxA was determined in the presence (+) and absence (-) of TCEP. Data represents the mean ± SE (n=3).

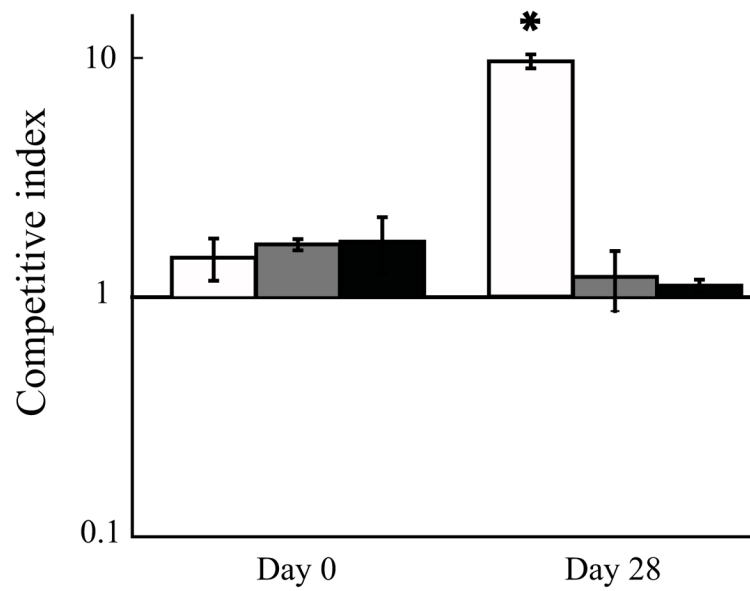


**FIGURE 7. CtpD is required for proper fitness of *M. tuberculosis* in a mix competition assay** Competitive index of each mutant relative to wild-type H37Rv was measured at 0 and 28 days post-infection in mice lungs. White bars, *ctpD::hyg* mutant vs. H37Rv; gray bars, *ctpJ::hyg* mutant vs. H37Rv; black bars, *ctpD::hyg* mutant complemented with plasmid pJEB402-D vs. H37Rv. Data are mean  $\pm$  SE (n=3). \*p<0.05 vs. post-infection day 0.

Table 1

List of primers used in this work.

Name	Sequence	Use
qctpD-F	GCCGCCATCGTCTTGTTG	qPCR of <i>ctpD</i>
qctpD-R	GCATCCGGACGAAGCTGATC	qPCR of <i>ctpD</i>
qctpJ-F	CGGCATCTGGGTGTACGAA	qPCR of <i>ctpJ</i>
qctpJ-R	TGGGTGCTCACTGGGATAAC	qPCR of <i>ctpJ</i>
qsigAMtb-F	CTCGGTTTCGGCCTACCTCA	qPCR of <i>sigA</i>
qsigAMtb-R	GCGCTCGCTAAGCTCGGTCA	qPCR of <i>sigA</i>
For-ctpD	ATGACCTTGACCGCTGTGAAG	Clone <i>ctpD</i> + TEV in pBAD
Rev-TEV-D	CGCGGCTTCGGCTGCGCGTAGCAGCGGCGAAAACCTGTATTTTCAGTCC	Clone <i>ctpD</i> + TEV in pBAD
For-ctpJ	GTGGCTGTTCGTGAACTCTCTC	Clone <i>ctpJ</i> + TEV in pBAD
Rev-TEV-J	CGTGGCACCCGCGCACAGGAGCAGCGGCGAAAACCTGTATTTTCAGTCC	Clone <i>ctpJ</i> + TEV in pBAD
For-TrxA	ATGACCACTCGAGACCTCAC	Clone <i>trxA</i> + TEV in pEXP5-CT
Rev-TEV-TrxA	CCTGGAACAAAGACTTCATCCAGCAGCGGCGAAAACCTGTATTTTCAGTCC	Clone <i>trxA</i> + TEV in pEXP5-CT
F-ctpJ-EcoRI	AGCTGAATTCGTGGCTGTTCGTGAACTCTCTC	Clone <i>ctpJ</i> in pJEB402 under <i>mop</i> promoter regulation
R-ctpJ-HpaI	GACTGTAACTCACCTGTGCGGGTGCCAGC	Clone <i>ctpJ</i> in pJEB402 under <i>mop</i> promoter regulation
prEL4-ctpD forward	ATTCTAGACGATGATTAGCGCGCCAAC	Clone <i>ctpD</i> in pJEB402 under <i>mop</i> promoter regulation
prEL6-ctpD reverse	ATGGTACCAGCGTGGCAACAACCTTGAC	Clone <i>ctpD</i> in pJEB402 under <i>mop</i> promoter regulation
F-5UTR-ctpJ	ACTGGCGGCCGCGACCAAGGTGCAAGTGCTCGCTG	Clone 400 pb upstream <i>ctpJ</i> including first 100 bp of the gene
R-5UTR-ctpJ	CAGTACTAGTCCCAACGCATCTCCGACAACGC	Clone 400 pb upstream <i>ctpJ</i> including first 100 bp of the gene
F-3UTR-ctpJ	ACTGCTCGAGCGCCGACACGAAGGTTCCACC	Clone 400 pb downstream <i>ctpJ</i> including last 100 bp of the gene
R-3UTR-ctpJ	CAGTGGGCCCAGCGAGCGTCTCGGTGGACC	Clone 400 pb downstream <i>ctpJ</i> including last 100 bp of the gene
For-1469	ACGATCATCGGGTTGGCACG	<i>ctpD</i> genetic environment
Rev-1470	GTCAAAGTGTTCCGCGACG	<i>ctpD</i> genetic environment
For-1470	CGAGAAAGATCTGGCCTCG	<i>ctpD</i> genetic environment
Rev-1471	CGCTGCAAGCTCTCGTTC	<i>ctpD</i> genetic environment
For-1471	GAACGAGAGCTTGCAGCG	<i>ctpD</i> genetic environment
Rev-1472	CGCTAAGGCCTCTTTGAGC	<i>ctpD</i> genetic environment
For-1472	GATGAACAGCTGCTAGATGC	<i>ctpD</i> genetic environment
Rev-1473	CTTCTCCAGATCAGTGAGC	<i>ctpD</i> genetic environment

Table 2

Metal binding stoichiometry of His-less CtpD and CtpJ.

<u>Protein</u>	<u>Co<sup>2+</sup> protein molar ratio<sup>a</sup></u>		<u>Ni<sup>2+</sup> protein molar ratio<sup>a</sup></u>	
	<u>No vanadate</u>	<u>1.5 mM vanadate</u>	<u>No vanadate</u>	<u>1.5 mM vanadate</u>
CtpD	1.08 ± 0.14	0.35 ± 0.02	1.04 ± 0.05	0.38 ± 0.08
CtpJ	1.06 ± 0.27	0.05 ± 0.01	0.92 ± 0.13	0.28 ± 0.03

<sup>a</sup> Stoichiometry was estimated as moles metal : moles CtpD. Metal content in protein was determined by furnace AAS.